AIAA JOURNAL
Vol. 34, No. 8, August 1996

Technical Notes

TECHNICAL NOTES are short manuscripts describing new developments or important results of a preliminary nature. These Notes cannot exceed 6 manuscript pages and 3 figures; a page of text may be substituted for a figure and vice versa. After informal review by the editors, they may be published within a few months of the date of receipt. Style requirements are the same as for regular contributions (see inside back cover).

Multiaxis Fluidic Thrust Vector Control of a Supersonic Jet Using Counterflow

D. M. Washington* and F. S. Alvi†
Florida A&M University and Florida State University, Tallahassee, Florida 32310
P. J. Strykowski‡
University of Minnesota, Minneapolis, Minnesota 55455
and
A. Krothapalli§
Florida A&M University and Florida State University, Tallahassee, Florida 32310

Introduction

FLIGHT tests have demonstrated the performance advantages of using thrust vector control over more traditional approaches that rely on aerodynamic surfaces for maneuverability. Thrust vector control of high-performance fighter aircraft has been shown to improve control and agility at high-angle-of-attack conditions as well as at low speeds where aerodynamic surfaces are relatively ineffective. Furthermore, it is envisioned that thrust vector control may eliminate much of the vertical and horizontal tail structure of the aircraft, reducing weight and radar cross signature.

Current thrust-vectoring technologies have focused on both two-dimensional pitch-vectoring systems as well as axisymmetric multiaxis vectoring nozzles. However, these promising concepts require complicated hardware to redirect the engine exhaust, adding considerable weight to the aircraft and imposing limitations in terms of jet dynamic response and nozzle cooling. Although recent advances have been made in developing lightweight, multiaxis vectoring nozzles with low external drag,[1,2] design challenges at the system integration level still exist that must overcome the actuation-and-control hardware requirements needed to redirect the engine exhaust by mechanical means.

A different approach to jet thrust vectoring—commonly referred to as fluidic control—uses one or more secondary airstreams to redirect the primary jet, thereby achieving thrust vector control in the absence of moving surfaces. Early studies of fluidic control[3] demonstrated that small secondary jets could be used effectively to control the vector response of the primary flow. Although large vector angles could be achieved in this fashion, nonhysteretic jet response was possible only over a very limited portion of the operating domain, seriously reducing the likelihood that the technology would be viable in aircraft applications.

A relatively new fluidic control technique, which employs secondary flow traveling in a direction opposite to the primary jet—namely, counterflow control—has been explored by Strykowski et al.[4] at jet Mach numbers up to 2. These studies conclusively show that the primary jet can be continuously vectored up to angles approaching 20 deg. Furthermore, if implemented correctly, counterflow thrust vectoring (CFTV) does not suffer from the bistability problems encountered with earlier fluidic control schemes. We describe the results of a study in which a Mach 2 diamond-shaped jet was used to extend the single-axis vectoring concept of rectangular jets to multiaxis operation.

Facilities

The experiments were conducted in the blowdown compressed-air facility of the Fluid Mechanics Research Laboratory at Florida State University, which is capable of supplying hot and cold air to drive the primary jet. The Mach 2 diamond-shaped nozzle used for the experiment was designed to have the same throat and exit area as the rectangular nozzle used for the supersonic study[4]; details of the diamond jet can be found elsewhere.[5] The stagnation-to-ambient-pressure ratio across the nozzle was fixed to achieve isentropically expanded flow at Mach 2. The jet was operated cold at a stagnation temperature of 300 K with $Re = 1.23 \times 10^6$, based on the short dimension of the jet.

To achieve CFTV a secondary airstream must be established along the outer surface of one of the jet shear layers. This secondary stream is created by connecting a vacuum source to a chamber placed along the periphery of the jet; details of this arrangement are discussed later. The thrust vector response using counterflow was quantified using planar laser scattering (PLS) imaging of the flow. The laser sheet was oriented along the diamond jet axis in the plane in which the jet was vectored. Submicron ice crystals are formed because of the condensation of the moist ambient air entrained into the shear layers at the periphery of the cold jet. These ice crystals scatter the light from the laser sheet, thus rendering the jet shear layers visible.

Results

Recent studies of pitch vectoring using counterflow indicate that the amount of secondary flow required to achieve a desired thrust vector angle is inversely proportional to the area of the shear layer along which the secondary flow is applied.[4] For this reason, the diamond nozzle was selected as a candidate geometry with which to demonstrate multiaxis thrust-vectoring capability. In contrast to the 4:1 aspect-ratio rectangular jet studied previously, which produced only two shear layers of significant size along which counterflow could be established, the diamond jet is bounded by four shear layers of equal size. Accordingly, by creating a secondary counterflowing stream along the outer periphery of any of the four shear layers, the jet can, in principle, be vectored in the direction normal to the shear layers, providing multiaxis control.

Side-view and end-view schematics of the counterflowing nozzle-collar assembly and the diamond nozzle are shown in Fig. 1. The side view also indicates the conditions necessary to achieve jet vectoring at an angle δ_v as a result of the secondary counterflow that is established along the upper shear layer. The collar provides four gaps at the nozzle exit, between the nozzle and the collar, through which suction can be applied. When the vacuum system connected to a particular chamber of the diamond nozzle (labeled A–D in Fig. 1)

Received Nov. 20, 1995; revision received April 18, 1996; accepted for publication April 18, 1996.

*Graduate Research Assistant, Fluid Mechanics Research Laboratory, Department of Mechanical Engineering.
†Assistant Professor, Fluid Mechanics Research Laboratory, Department of Mechanical Engineering. Member AIAA.
‡Associate Professor, Department of Mechanical Engineering. Member AIAA.
§Don Fuqua Professor, Departmental Chairman, Fluid Mechanics Research Laboratory, Department of Mechanical Engineering. Associate Fellow AIAA.

is activated, a secondary counterflowing stream is created within the gap defined by the collar surface and the corresponding shear layer of the jet. The collar was designed such that the counterflow stream is applied, in principle, to only one of the shear layers and isolated from the other three, a requirement of the CFTV technique. Nozzle-collar design parameters, such as gap height, collar length, and collar curvature, chosen in the present study of the diamond jet, were taken from the performance predictions based on earlier studies of single-axis CFTV nozzles.[4] The diamond-jet collar design was chosen to produce a jet deflection angle δ_v between 15 and 20 deg at maximum suction. As the subsequent discussion shows, this design approach was reasonably successful.

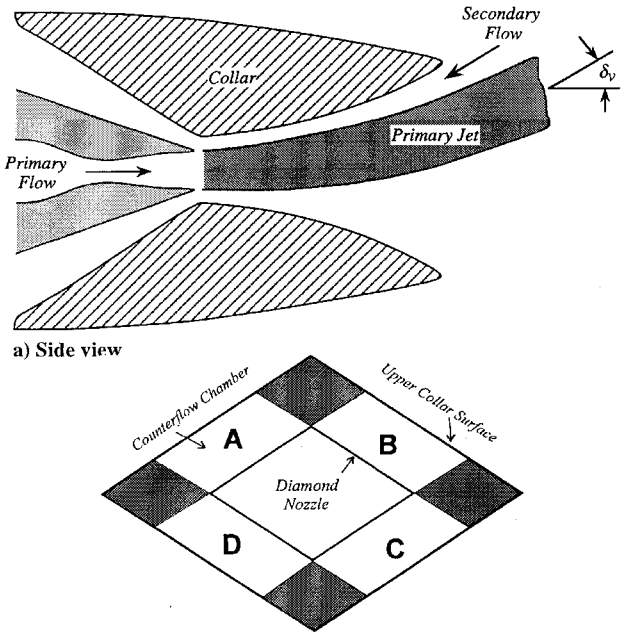

a) Side view

b) End view

Fig. 1 Schematic of multiaxis fluidic thrust vector nozzle and collar geometry.

Instantaneous PLS images showing cross-sectional views of the unvectored and vectored diamond jet are presented in Figs. 2a and 2b, respectively. No suction has been applied for the unvectored case shown in Fig. 2a, whereas Fig. 2b corresponds to the case with maximum suction/counterflow in chamber C, where the jet has clearly been vectored into that chamber. Note that the unvectored jet in Fig. 2a appears to be off-center because of the oblique viewing angle of the camera. The large vectoring angles that can be achieved using multiaxis CFTV are perhaps more dramatically displayed in the side-view images shown in Figs. 2c and 2d. Figure 2c depicts the unvectored jet with no suction, and Fig. 2d shows the jet at maximum deflection ($\delta_v \sim 15$ deg).

We were able to continuously vector the diamond jet into any of the four chambers by establishing counterflow via suction in the desired chamber, results similar to those obtained in the single-axis study.[4] The relationship between the degree of counterflow and jet deflection was explored by varying the suction pressure and measuring the jet deflection angle from side-view PLS images. A summary of the diamond-jet vectoring angles δ_v as a function of the counterflow static-pressure parameter is provided in Fig. 3. The static-pressure parameter is the leading order term obtained from a control volume analysis of the nozzle-collar system for ideally expanded jets, details of which can be found elsewhere.[4] The parameter is essentially a nondimensional ratio of the side force acting on the jet, represented by $\Delta \boldsymbol{P}_{\text{exit}} \cdot \boldsymbol{A}_{\text{side}}$, and the axial force imposed by the jet $\rho_1 U_1^2 \cdot \boldsymbol{A}_{\text{jet}}$. The pressure $\Delta \boldsymbol{P}_{\text{exit}}$ represents the vacuum pressure established in the secondary stream as measured in the jet exit plane and increases as the counterflow is increased.

For completeness, data from the single-axis rectangular jet experiment[4] also are included in Fig. 3. The upper curve represents

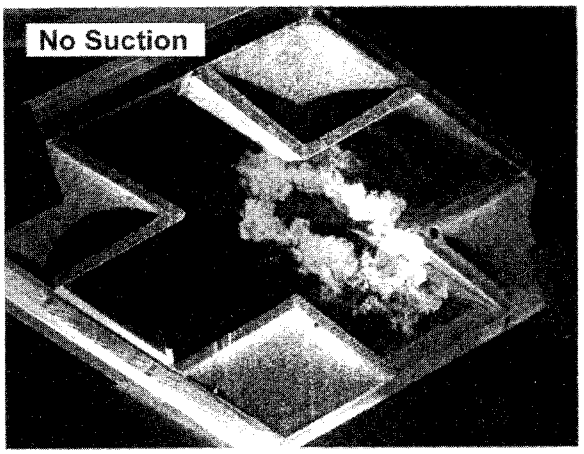

a) Cross-sectional view, unvectored jet

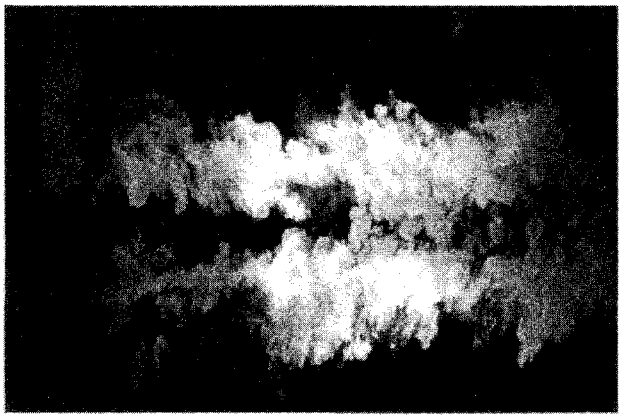

c) Side view, unvectored jet

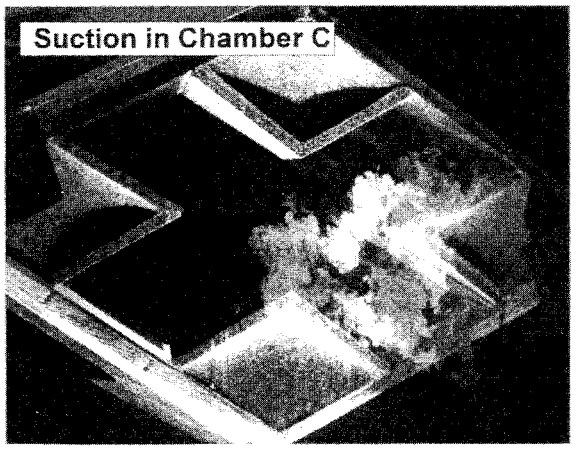

b) Cross-sectional view, jet vectored into chamber C

d) Side view, jet vectored to approximately 15 deg

Fig. 2 PLS images of vectored and vectored diamond jet.

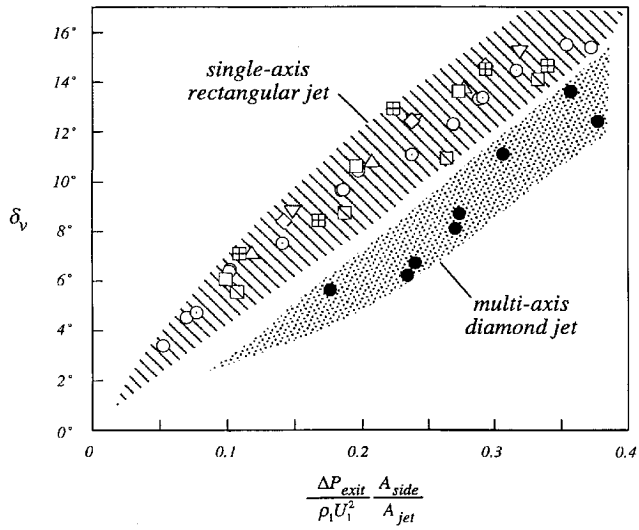

Fig. 3 Thrust vector response curves for Mach 2 jets.

the single-axis CFTV results and includes data for hot and cold jets measured over a range of collar design parameters, i.e., various collar lengths and suction gap heights. Estimates of δ_v for the single-axis study were obtained using a control volume analysis including integrated pressure profiles measured along the collar surface as well as flow visualization images using the PLS technique employed in the present study. Within experimental uncertainty, the single-axis data essentially collapse onto a single curve displaying an approximately linear dependence on the nondimensional pressure parameter. The good collapse of the single-axis thrust vector data over a wide parametric range indicates that the scaling in Fig. 3 captures the essential features of the pressure forces and momentum fluxes contained in a complete control volume analysis applied to the jet-nozzle system. Furthermore, the agreement between the vectoring angles obtained using a control volume analysis and those estimated using PLS images indicates the reliability of optical techniques for measuring δ_v.

The data for the current multiaxis study are shown in the lower curve, where the scatter and the uncertainty in the measurements are roughly indicated by the shaded region. As in the single-axis study, the jet thrust vector angle is almost linearly proportional to the amount of counterflow. At the maximum suction pressure of approximately 7.5 psia—a pressure limitation primarily imposed by the efficiency of the vacuum system—a maximum deflection angle of approximately 15 deg was obtained. The mass flux rates of the counterflowing stream were too low to be accurately measured in the present study. However, similar meaurements made in the Mach 2 rectangular jet[4] suggest that the counterflow mass flux is well below 2% of the primary jet flow for all cases shown in Fig. 3.

Although the multiaxis data show reasonably linear behavior, similar to the performance of a single-axis system, the curves for the two cases are distinct and the single-axis geometry appears to be slightly more efficient. We believe that the primary reason for the differences in thrust vector performance of the single- and multiaxis systems is attributable to a noticeable leakage between adjacent chambers of the collar assembly of the diamond jet. This was determined by monitoring the static-pressure distributions in the four chamber of the dimond nozzle. Leakage effects indicate that counterflow is not confined to a single shear layer of the diamond jet, resulting in a degradation of performance principally attributable to the transverse pressure gradient across the shear layer. Although these three-dimensional effects undoubtedly will influence the collar performance, we believe that they can be minimized by improvements in collar design. The collar design was not optimized in the present study, where the goal was to demonstrate the proof of concept of a multiaxis thrust vector system based on fluidic control.

Conclusions

Fluidic thrust vector control was examined in a Mach 2 diamond nozzle to determine the efficacy of multiaxis control using counterflow. The results clearly demonstrate that a secondary counterflowing stream applied along the periphery of the primary shear layer can be used effectively to achieve nonhysteretic thrust vector control in multiaxes and up to angles approaching 15 deg. These results are an extension of previous studies where CFTV was applied to single-axis pitch control at Mach numbers up to 2 and indicate the robustness of the CFTV concept, which has many attractive features including the elimination of mechanical control surfaces and the inherent film cooling made possible by the ambient counterflow.

Acknowledgments

Support for this research was provided by the U.S. Office of Naval Research (Contract N00014-92-J-1406) and NASA (Contract NAG-2930).

References

[1]Snow, B. H., "Thrust Vectoring Control Concepts and Issues," Society of Automotive Engineers TP Ser. 901848, 1990.

[2]Capone, F., Smereczniak, P., Spetnagel, D., and Thayer, E., "Comparative Investigation of Multiplane Thrust Vectoring Nozzles," AIAA Paper 92-3264, July 1992.

[3]Warren, R. W., "Some Parameters Affecting the Design of Bistable Fluid Amplifiers," ASME Symposium on Fluid Jet Control Devices, Winter Annual Meeting, American Society of Mechanical Engineers, Nov. 1962, pp. 75–82.

[4]Strykowski, P. J., Krothapalli, A., and Forliti, D. J., "Counterflow Thrust Vectoring of Supersonic Jets," AIAA Paper 96-0115, Jan. 1996; also, *AIAA Journal* (submitted for publication).

[5]Alvi, F. S., Krothapalli, A., Washington, D., and King, C. J., "Aeroacoustic Properties of a Supersonic Diamond-Shaped Jet," *AIAA Journal*, Vol. 34, No. 8, 1996, pp. 1562–1569.

Three-Dimensional Velocity Measurements Within Görtler Vortices

J. A. Rothenflue* and P. I. King†
U.S. Air Force Institute of Technology, Wright–Patterson Air Force Base, Ohio 45433

Introduction

IN 1940, Görtler[1] predicted that streamwise-oriented, counter-rotating vortices would develop in response to the centrifugal instability within a laminar boundary layer over a concave surface. Hot-wire[2] and laser Doppler[3] anemometry (LDA) have been used to detect Görtler vortices (GVs) through spanwise periodic variations in the streamwise velocity component within the boundary layer; however, cross-stream velocity component measurements within the vortices have remained conspicuously absent from the literature.

Obtaining cross-stream velocity measurements within GVs is difficult because of the weak nature of the disturbance. A GV in a laminar boundary layer is, in reality, little more than a small twist of the fluid, typically turning through no more than 90 deg before breakup as a result of boundary-layer transition to turbulence.[4] A coordinate system and geometry for a typical set of GVs are depicted in Fig. 1, where R is the radius of curvature of the surface, δ is the boundary-layer thickness, and U is the freestream velocity.[5] The u, v, and w velocity components are the local flow velocities in the x, y, and z directions, respectively.

Received Jan. 6, 1995; revision received Jan. 2, 1996; accepted for publication April 15, 1996. This paper is declared a work of the U.S. Government and is not subject to copyright protection in the United States.

*Doctoral Candidate; currently Deputy for Technology Transfer, Applied Laser Technology Branch, U.S. Air Force Phillips Laboratory, 3550 Aberdeen Avenue, SE Building 619, Kirtland Air Force Base, NM 87117-5776. Member AIAA.

†Associate Professor, Department of Aeronautics and Astronautics, 2950 P Street. Senior Member AIAA.